1   **Title page**

2    **Establishing human leukemia xenograft mouse models by implanting human bone marrow-**

3                          **like scaffold-based niches**

4

5   **Short Title:** Establishing a human leukemia xenograft mouse model

6

7   Antonella Antonelli[1], Willy A Noort[2], Jenny Jaques[1], Bauke de Boer[1], Regina de Jong-Korlaar[2],

8   Annet Z Brouwers-Vos[1], Linda Lubbers-Aalders[2], Jeroen F van Velzen[3], Andries C Bloem[3],

9   Huipin Yuan[4], Joost D de Bruijn[5], Gert J Ossenkoppele[2], Anton CM Martens[2], Edo Vellenga[1],

10  Richard WJ Groen[2*], and Jan Jacob Schuringa[1*]

11

12  [1]Department of Experimental Hematology, Cancer Research Center Groningen (CRCG),

13  University Medical Center Groningen, University of Groningen, The Netherlands. [2]Dept of

14  Hematology, VU University Medical Center, Amsterdam, The Netherlands. [3]Dept of Immunology,

15  University Medical Center Utrecht, Utrecht, The Netherlands. [4]Xpand Biotechnology BV,

16  Bilthoven, The Netherlands. [5]Queen Mary University of London, School of Engineering and

17  Materials Science (SEMS), Mile End Road, E1 4NS London, UK.

18  * Corresponding authors

19

1   **Full name, mailing address and email of corresponding authors:** J.J. Schuringa, Department of

2   Experimental Hematology, Cancer Research Center Groningen (CRCG), University Medical

3   Center Groningen, University of Groningen, Hanzeplein 1, DA13, 9700RB, Groningen, The

4   Netherlands. Phone: +31-503619391, fax: +31-503614862, email: j.j.schuringa@umcg.nl; and

5   R.W.J. Groen, Department of Hematology, VU University Medical Center, De Boelelaan 1117,

6   PK2 BR012, 1081HV, Amsterdam, The Netherlands. Phone: +31-204442345, fax: +31-

7   204442601, email: r.groen@vumc.nl

8

9   **Word count: 3993**

10   **Total number of figures: 6**

11   **Total number of Tables: 0**

12

**Key points**

1. Humanized niche xenograft mouse models were generated that enable engraftment of leukemia patient cells covering all risk groups

2. Self-renewal is better maintained in the humanized niches as determined by serial transplantation and genome-wide transcriptome studies

1

2 **Abstract**

3

4 In order to begin to understand mechanisms that regulate self-renewal, differentiation and

5 transformation of human hematopoietic stem cells, or to evaluate the efficacy of novel treatment

6 modalities, stem cells need to be studied in their own species-specific microenvironment. By

7 implanting ceramic scaffolds coated with human mesenchymal stromal cells (MSCs) into immune

8 deficient mice we mimic the human bone marrow niche. Thus, we have established a human

9 leukemia xenograft mouse model in which a large cohort of patient samples successfully engrafted

10 covering all important genetic and risk subgroups. We find that by providing a humanized

11 environment stem cell self-renewal properties are better maintained as determined by serial

12 transplantation assays and genome-wide transcriptome studies, and less clonal drift is observed as

13 determined by exome sequencing. The human leukemia xenograft mouse models that we have

14 established here will serve as an excellent resource for future studies aimed at exploring novel

15 therapeutic approaches.

16

17

18

19

# Introduction

In order to study the molecular mechanisms involved in human leukemias and to improve treatment options, establishing *in vivo* xenograft models that faithfully recapitulate the disease is essential. Currently, NOD-SCID IL2Rγ$^{-/-}$ (NSG) xenograft models are considered to be the gold standard for evaluating engraftment of human haematological malignancies. However, this model has serious drawbacks since 30-40% of primary AML samples fail to engraft even in this most immune-compromised NSG model.[1-3] In addition, engraftment of normal human CD34$^{+}$ cells in NSG mice is lymphoid biased and *in vivo* myeloid transformation has been much more difficult to achieve in NOD-SCID based xenograft models, including the NSG mice.[4-8] Furthermore, using retro/lentiviral systems to model human leukemias we frequently observe that while *in vitro* both myeloid and lymphoid transformation can be achieved upon expression of oncogenes such as MLL-AF9 or BCR-ABL/BMI1, *in vivo* transformation in mice is strongly biased towards ALL.[5,6] This is in contrast to patients expressing the BCR-ABL p210 oncoprotein, which can give rise to both myeloid and lymphoid leukemias, and the same is true for MLL-AF9 in paediatric leukemia patients. Together, these observations suggest that a specific human microenvironment might be necessary for engraftment and maintenance of self-renewal of myeloid leukemic stem cells.

Since certain myeloid growth factors are often species-specific, the murine bone marrow niche is most likely not sufficient to provide the appropriate environment for human LSCs. NOD/SCID-3/GM/SF mice engineered to produce human IL3, GM-CSF and Steel Factor/SCF[9-11] and NOD-SCID IL2Rγ$^{-/-}$ (NSG) mice expressing human IL3, GM-CSF and SCF (NS-SGM3)[3] have been generated, and enhanced engraftability of primary human AML samples was observed in these mouse strains. Also, the expression of these three human growth factors was sufficient to allow AML development upon transplantation of CB CD34$^{+}$ cells expressing MLL-AF9.[3] Various other

5

1     mouse strains have also been developed[11-17] including MISTRG mice expressing M-CSF, IL3,

2     GM-CSF, TPO and SIRPα[12] and are therefore useful tools, although other human niche-specific

3     factors might still be missing.

4     To develop *in vivo* mouse leukemia xenograft models that would more faithfully recapitulate

5     human leukemias we made use of a humanized niche xenograft model in which ceramic scaffolds

6     coated with human mesenchymal stromal cells (MSCs) used to mimic the bone marrow

7     microenvironment are implanted in immunodeficient mice.[18,19] Next we studied the engraftment of

8     a large cohort of primary AML patient samples covering all important genetic and risk subgroups.

9     Our data indicate that the presence of a humanized microenvironment favors engraftment of AML

10     patient samples, including favorable risk AML samples that are notoriously difficult to engraft in

11     NSG strains and that self-renewal is better maintained in the human niche.

12

13     **Methods**

14     **Establishment of the humanized scaffold niche xenograft model and transplantations**

15     The ectopic bone model was established as described previously.[18,19] Briefly, four to six hybrid

16     scaffolds consisting of three 2–3mm biphasic calcium phosphate (BCP) particles loaded with

17     human MSCs were implanted subcutaneously into female NOD.Cγ-Prkdcscid Il2rγtm1Wjl/SzJ

18     (NSG) or RAG2$^{-/-}$γc$^{-/-}$ mice. Eight weeks after scaffold implantation, different cell doses ranging

19     from $5\times10^4$ to $4\times10^6$ were directly injected into the scaffolds as indicated during primary as well as

20     secondary transplantations.

21

22     **Patient samples**

1 Peripheral blood and bone marrow from untreated patients diagnosed with AML/ BC-CML/ B-

2 ALL at the UMCG or VUmc were studied after informed consent and protocol approval by the

3 Medical Ethical Committee of the UMCG or VUmc, in accordance with the Declaration of

4 Helsinki. After ficoll separation of mononuclear cells, cells were cryopreserved until further use.

5 CD34+ cells were enriched or CD3+ cells were depleted using a magnetically activated cell-sorting

6 CD34 progenitor kit or automatically by using auto Macs (Miltenyi Biotech) as described

7 previously.[6,20]

8

9 **Additional Methods are described in the Supplemental Materials**

10

11 **Results**

12

13 **Establishing xenograft human leukemia models using three-dimensional scaffolds coated**

14 **with human MSCs.**

15 A cohort of 39 patients was selected to establish humanized niche mouse xenograft leukemia

16 models (Supplemental Table 1; 17/39 (44%) adverse risk group, 8/39 (21%) intermediate risk and

17 14/39 (36%) favorable risk). Cells were injected into a humanized model that is based on

18 subcutaneous implantation of human BM-like scaffolds (huBM-sc) in order to provide a human

19 microenvironment, as described previously.[18,19] Briefly, in this model ceramic scaffolds coated

20 with human mesenchymal stromal cells (MSCs) were implanted subcutaneous in immunodeficient

21 mice where they developed into structures mimicking a human bone marrow microenvironment

22 including bone formation, and ossicles were vascularized by murine blood vessels (Figure 1B,

23 Supplemental Figure 1, Supplemental Figure 2A). Six to eight weeks later, CD34+ or CD3+-

depleted AML mononuclear cells (MNCs) were then injected in these so-formed "ossicles". As comparator, 6 of the patient samples were also injected intravenously (i.v., referred to as muBM-iv) in mice without human scaffolds to evaluate engraftment in a murine microenvironment (Figure 1A, Supplemental Table 1). As second comparator, cells were injected either directly in the scaffold or i.v. in mice that did carry humanized scaffolds in 5 selected cases (referred to as IV huBM-sc, Figure 1A, Figure 1E). Experiments were carried out independently in two institutes using 2 different mouse strains, NSG (at the UMCG, NL) and $Rag2^{-/-}\gamma c^{-/-}$ mice (at the VU, NL) (Supplemental Table 1) showing robustness of the model. Leukemic cell engraftment was monitored over time with PB sampling and/or by monitoring tumor volume in the scaffolds (Figure 1A, Supplemental Table 2). Hematoxylin and Eosin (HE) staining of non-injected scaffold sections 6 weeks after implantation confirmed the presence of extramedullary bone in the scaffolds. Different magnifications reveal the presence of stromal cells and bone material deposited in the cavities of the ceramic particle, and blood vessels of mouse origin were also observed (Figure 1B, Supplemental Figure 1A, Supplemental Figure 2A).

For huBM-sc mice, chimerism levels in the PB were usually low (Supplemental Table 2), so the volume of the biggest tumor growing on one of the scaffolds at approximately 1.5-2 cm$^3$ was defined as endpoint of the experiment. MuBM-iv mice were terminated when we observed huCD45$^+$ levels in the PB around 30-60% of total living cells together with signs of illness. We obtained engraftment and outgrowth of leukemic cells in 3 out of 7 cases with the muBM-iv model (43%) and in 29 out of 39 cases (74%) in the huBM-sc model. Lack of engraftment was not due to an absence of bone formation in the scaffolds (Supplemental Figure 1B). Notably, favorable risk leukemias only engrafted in the huBM-sc model but no engraftment was observed in any of the muBM-iv mice without humanized scaffolds, and the same was true for patient sample #2 that also

did not engraft in the muBM-iv model (Figure 1C, Supplemental Table 1). All 7 favorable risk

AMLs with an inv16, which are notoriously difficult to engraft in NSG mice, efficiently engrafted

in the huBM-sc mice (Supplemental Table 1). AML #1  engrafted in both the huBM-sc as well the

muBM-iv models with similar kinetics of leukemia development, while AMLs #3 and #4 did

engraft in the muBM-iv model but with slower kinetics as compared to the huBM-sc model

(Supplemental Table 2).

All intermediate risk samples engrafted in both models (Figure 1C, Figure 1D). Interestingly, in

huBM-sc mice leukemic cells engrafted not only in the humanized scaffold niches but also seeded

into murine hematopoietic organs, with engraftment levels in murine compartments increasing

concomitantly with prognosis of disease (e.g. the percentage of human leukocytes in muBM ranged

from 4 to 20% in the favorable risk mice while chimerism levels in murine BM, spleen and liver

were significantly higher in mice injected with adverse risk samples reaching up to an average of

55% in one case of adverse risk leukemia) (Figure 1D). Five AML samples were i.v. injected in

mice carrying humanized scaffolds (Figure 1A, route 3). All samples efficiently seeded into the

scaffolds while only in 2/5 cases engraftment was also observed in the human bone marrow (Figure

1E).

The onset of tumor initiation and consequently the time of sacrifice (14-38 weeks) were variable

from patient to patient, with tumor growth rates that appeared to correlate with risk group. In the

majority of animals, tumors be palpable 100 days after injection with the exception of 2 cases of

adverse risk AML (#4 and #2) where the onset was earlier than 100 days (Figure 1F, Supplemental

Table 2). Furthermore, using a luciferase gene-marked AML sample, we observed that growth was

initiated 50 days after engraftment (Supplemental Figure 2C). In all cases of engrafted intermediate

1 and adverse risk leukemias, the growth rate (read out by the slope of the curve) was faster than in

2 favorable risk AMLs (Figure 1F, Supplemental Table 2).

3

4 **Leukemic cells engrafted in huBM-sc mouse models recapitulate the original phenotype of**

5 **the patient.**

6 FACS analysis was performed to compare the immunophenotype of the leukemic cells of the

7 original patient samples with tumor cells isolated from the human scaffold niche as well as from

8 the murine compartments. In some cases the original patient immunophenotype was well

9 conserved *in vivo* regardless of whether the cells expanded in a humanized or murine

10 microenvironment, while in other cases the original patient immunophenotype was clearly better

11 preserved in the humanized scaffolds. An example of the latter is AML #2. This sample contained

12 an inv16 and a t(9;22) BCR-ABL translocation with no mutations in NPM or FLT3. At

13 presentation, this patient displayed a relatively large immature population of blast cells (34%

14 CD34$^+$, 48% CD117$^+$ CD15$^-$ ) and all MNCs were positive for CD33 and CD13, weakly positive

15 for CD14, CD11b, CD11c and CD15, and negative for CD19 (Figure 2A). CD34$^+$ blast cells were

16 isolated from this patient and injected in the scaffolds of NSG mice and within 14 weeks tumors

17 developed on the scaffolds and the animals were terminated (Figure 2B, Supplemental Table 2).

18 Scaffold tumors were greenish in color (indicating the presence of myeloid myeloperoxidase

19 expressing cells) and were well vascularized with murine blood vessels. Leukemic cells could also

20 be retrieved from murine BM, spleen, liver and PB (Supplemental Table 2). Cells retrieved from

21 the humanized scaffolds were huCD45$^+$ with percentages of CD34$^+$ and CD117$^+$ comparable to the

22 percentages at diagnosis, whereas in cells retrieved from BM the percentage of CD34$^+$ and in

23 particular CD117$^+$ cells was partially reduced while CD15 and to some extent also CD11b and

1 CD14 percentages were increased (Figure 2C, Figure 2D). Histological analysis using HE staining

2 confirmed that scaffold tumors contained bone and huCD45$^{neg}$ stromal cells surrounded by

3 huCD45 and huCD33-positive AML blasts (Figure 2E). MGG staining of cytospins confirmed that

4 scaffold tumors mainly contained immature blast-like cells with big nuclei and BM samples

5 revealed a more abundant presence of smaller cells with a more differentiated morphology (Figure

6 2F).

7 In the case of AML #1, the humanized niche did not clearly confer an advantage to preserve a more

8 immature phenotype compared to the murine stromal environment (Supplemental Figure 3). This

9 sample contained a FLT3-ITD, was NPMwt and contained several chromosomal abnormalities

10 including a t(3;5) NPM-MLF1 translocation, with a high percentage of CD34$^{+}$/CD117$^{+}$ blasts

11 (Supplemental Figure 3A). Within 100-150 days tumors were visible and again infiltration of

12 human CD45$^{+}$ cells was observed in mouse organs as well (Supplemental Figure 3B-C,

13 Supplemental Table 2). However, the immunophenotype of the original patient sample #1 was now

14 conserved in both the humanized niche as well as in mouse niches (Supplemental Figure 3C-F).

15

16 **Leukemic cells isolated from humanized scaffolds have superior 2$^{nd}$ transplantation capacity**

17 **compared to leukemic cells isolated from the murine bone marrow niche.**

18 Secondary transplantation assays were performed for three cases using various doses ranging from

19 $4.5x10^4$-$3x10^6$ cells harvested from scaffolds or bone marrow that were injected into individual

20 scaffolds of secondary mice (Figure 3A). Secondary engraftment transplantation into 2$^{nd}$ scaffolds

21 could readily be established for huBM-sc-harvested cells in all investigated cases (Figure 3A-G

22 and Supplemental Figure 2D). For AML #2 secondary transplantation could readily be established

23 for huBM-sc-harvested cells with $3x10^6$, $1x10^6$ and even $4x10^5$ cells, but no 2$^{nd}$ engraftment was

1   observed for muBM-iv-harvested cells using up to $4 \times 10^5$ cells (Figure 3B-C, Supplemental Table

2   2). The same was true for AML #3 whereby $2^{nd}$ engraftment was observed with $1.5 \times 10^6$ and $1 \times 10^5$

3   injected huBM-sc-harvested cells, but not with up to $4 \times 10^5$ muBM-iv-harvested cells  (Figure 3D-

4   E, Supplemental Table 2). For AML #1, $2^{nd}$ engraftment could be established with as little as

5   $4.5 \times 10^4$ huBM-sc-harvested cells, which was not seen with muBM-iv-harvested cells when

6   injected at the same dose, but injection of $1.8 \times 10^5$ muBM-iv-harvested cells did allow secondary

7   transplantation, albeit with slower kinetics as compared to huBM-sc-harvested cells at the same

8   dose (Figure 3F-G, Supplemental Table 2). These data appeared to be in line with flow cytometry

9   analyses on stem/progenitor compartments suggesting that the immature $CD34^+/CD38^-$

10  compartments were better preserved in the human niches (Supplemental Figure 4A). Together,

11  these data again pinpoint to the notion that stemness was better preserved in the humanized niche

12  for most leukemias, whereby AML #1 seemed to be the least dependent on a human

13  microenvironment within the tested cohort, in line with our observation that this patient sample

14  was also able to engraft in the muBM-iv model, while e.g. AML #2 appeared to be much more

15  dependent on cues from a human microenvironment. We also analyzed lymphoid engraftment, but

16  did not find any $CD3^+/CD4^+$ or $CD3^+/CD8^+$ cells (Supplemental Figure 4B).

17  Next, we compared engraftment of a favorable risk, intermediate risk and adverse risk sample in

18  mice carrying scaffolds coated with either human MSCs or murine MSCs and performed primary

19  and secondary engraftment experiments (Figure 4A). The adverse risk sample engrafted in both

20  conditions, regardless of whether scaffolds were coated with human or murine MSCs (Figure 4B).

21  The intermediate risk sample showed the highest chimerism levels in scaffolds coated with human

22  MSCs compared to murine MSCs, and secondary engraftment was only observed with cells

23  harvested from human scaffolds (Figure 4B). Finally, the favorable risk sample efficiently

1 engrafted in the human scaffolds, and only at very late timepoints in the murine scaffolds (day 322)

2 (Figure 4B). Efficient secondary transplantation was observed in all three cases in mice carrying

3 scaffolds coated with human MSCs. No significant differences were seen in secondary

4 transplantation of adverse risk sample #27 when scaffolds coated with human versus murine MSCs

5 were compared, but significantly delayed secondary engraftment was observed with intermediate

6 risk sample #18 in the scaffolds coated with murine MSCs. Failure of engraftment in the murine

7 scaffolds was not due to insufficient formation of an extramedullary murine niche development

8 (Figure 4D).

9

10 **Evaluation of clonal heterogeneity and clonal drift within humanized and murine niches.**

11 We selected three cases (#1, #2 and #3) in order to evaluate clonal heterogeneity and clonal drift.

12 Variant allelic frequencies (VAF, exome seq) of recurrent mutations were determined in patient

13 samples at presentation, and in tumor material harvested from the humanized scaffold niche, from

14 the murine BM niche, and from *in vitro* expanded AML on MS5 bone marrow stromal cells

15 supplemented with human cytokines. For #2 the CD34$^+$ fraction of the patient, two huBM-sc

16 samples, one muBM sample and *in vitro* expanded sample could be analyzed. As shown in Figure

17 5A, a number of mutations were detected with approximately 50% VAF, including XBP1, APC,

18 RPTOR, FLNC and MLL2 mutations, which were detected at the start, in the huBM-sc samples as

19 well as in the in vitro expanded  sample. In all these cases, the inv16 and t(9;22) translocation were

20 detected as well (data not shown). In contrast, these mutations were not detected in the muBM

21 expanded sample, which had lost the inv16, t(9;22) and mutations indicated above, but instead

22 displayed IDH1 mutations with an VAF of 50% which was only detected at low percentage in the

23 diagnostics sample, and various other mutations that had remained below the detection limit in the

1  diagnostic sample (Figure 5A), clearly indicating a change in clonal composition in the absence of

2  a humanized microenviroment. For AML #1 this clonal drift was not seen, although a small clone

3  or clones appeared with mutations in e.g. BCOR, KDM6A, PTPN11 and APC in the muBM that

4  was not detected at diagnosis or in the huBM-sc samples, while at day 43 in the *in vitro* expanded

5  cells again a different clone(s) appeared with mutations in HDAC7, IKZF1, MLL and XBP1

6  (Figure 5B). In sample #3 the main clone(s) with approximately 50% VAF in NRAS, MSH6,

7  DNMT3A was present at diagnosis and in the huBM-sc as well as the muBM samples. The

8  diagnosis sample also contained mutations in MUTYH and PLCG2 with a VAF of approximately

9  50% that was also seen in the huBM-sc sample but only at a very low VAF in the muBM sample

10  suggesting that this was an independent clones that did not efficiently grow out in the murine

11  niche. Finally, new small clone(s) appeared as well with low VAF in both the huBM-sc and muBM

12  samples that were not detected in the diagnostic sample (Figure 5C). Together, these data clearly

13  indicate that clonal heterogeneity and clonal drift are important parameters to evaluate in *in vitro*

14  and *in vivo* models, and that a humanized niche might be better suited to maintain clonal

15  heterogeneity observed at diagnosis.

16

17  **Human MSCs are better in supporting long-term expansion of human AML compared to**

18  **murine bone marrow stroma.**

19  *In vitro* experiments were performed using either human MSCs, murine MS5 bone marrow stromal

20  cells or liquid culture without stroma using #2 and #1 as representative examples. In all cases,

21  CD34$^+$-sorted AML cells were grown with or without a cocktail of human cytokines IL3, G-CSF

22  and TPO as we previously described.[21-23] No long-term cultures could be established without

23  stroma, although some expansion was observed for #2 in liquid-culture conditions with cytokines,

1 but within 20 days cells differentiated and stopped expanding (Supplemental Figure 5A). Human

2 MSCs clearly were superior in supporting long-term expansion of both AML samples even in the

3 absence of additional cytokines (Supplemental Figure 5A). The addition of cytokines did further

4 enhance expansion in both murine MS5 as well as in human MSC cocultures, but the immature

5 CD117$^+$ phenotype was clearly better preserved in the absence of cytokines, in particular for AML

6 #2 and to a lesser degree for AML #1 (Supplemental Figure 5B-C).

7

8 **Stemness transcriptome signatures are better preserved in a humanized niche.**

9 Transcriptome studies were performed on diagnostic samples as well as on huBM-sc and muBM

10 derived samples from leukemic mice for 6 patient samples (Supplemental Table 3). Unsupervised

11 hierarchical cluster analysis revealed that each patient displayed a unique transcriptome signature

12 regardless of where cells were retrieved from (huBM-sc, muBM or diagnostic sample) (Figure 6A).

13 Supervised clustering within individual patient samples revealed that diagnostic samples clustered

14 most closely together with the huBM-sc samples for AML cases #2, #3, #6 and #4 (Figure 6B).

15 This was not the case for AML #1 for which we had indeed already observed that this sample was

16 less dependent on a human environment for its self-renewal and stemness properties, and also for

17 the B-ALL sample #5 (Figure 6B). Gene Ontology (GO) analyses revealed that specific gene sets

18 were differently regulated in the human versus murine niche, including processes such as

19 transcription regulation, immune response, inflammatory response, mitochondria, and regulation of

20 apoptosis (Figure 6C). In line with our secondary transplantation studies, GSEA analyses revealed

21 significant enrichment for Leukemic Stem Cell signatures for #2 and #3 when grown in the

22 humanized scaffold compared to the murine BM, while this was not observed for sample #1

23 (Figure 6D). Instead, a significant enrichment for leukemic-GMP signatures was observed (Figure

1    6D). Examples of gene expression of individual genes are shown in Figure 6E, indicating that

2    expression of stem cell-related genes such as BMI1, HOXA5, HOXA9, CD34, CDKN1C and

3    GATA2 was better preserved in the human niche compared to the murine niche for AML #2, while

4    this was much less explicit for AML #1.

5
6

7    **Discussion**

8    Hematopoietic stem cells, and the same holds true for leukemic stem cells, do not simply live

9    alone.  They are surrounded by a variety of other cell types that together constitute the stem cell

10   niche in the bone marrow.[24-28] In order to begin to understand mechanisms that regulate self-

11   renewal, differentiation and transformation of human hematopoietic stem cells, both intrinsic

12   mechanisms as well as extrinsic mechanisms involving cues from the environment need to be taken

13   into account.[29,30]    Even though the currently available immune deficient NSG xenograft mouse

14   models are considered the gold standard for evaluating engraftment of human haematological

15   malignancies, these models have serious drawbacks since only a limited percentage of primary

16   AML patient samples can engraft and these models are strongly lymphoid biased.[1-8] Clearly, a

17   human bone marrow microenvironment that would provide a suitable home for normal and

18   leukemic stem cells is lacking in these animals. To capture and maintain stem cell self-renewal

19   programs and clonal heterogeneity as is observed in patients, a human niche appears to be essential.

20   By making use of scaffolds coated with human MSCs to create a humanized environment in mice

21   we have established human xenograft mouse leukemia models that can serve as a resource for

22   leukemic stem cell studies and the evaluation of novel therapeutic approaches. We find that by

23   providing a humanized environment: i) 29 out of 39 (74%) leukemia cases could efficiently engraft

24   in the huBM-sc model covering all important genetic subtypes and risk groups, whereby also all

16

1    favorable risk inv(16) patient samples could engraft, which are notoriously difficult to engraft in

2    NSG mice; ii) stem cell self-renewal is better preserved in essentially all investigated cases in the

3    huBM-sc as compared to the mouse bone marrow niche as determined by serial transplantation

4    assays; iii) clonal heterogeneity as observed in the original patient is much better preserved in the

5    huBM-sc compared to the mouse BM, at least in one case; and iv) stem cell self-renewal signatures

6    are better preserved in the huBM-sc in the majority of cases. Even when cells were injected i.v. in

7    mice carrying human scaffolds, better engraftment was observed in all 5 studied cases, whereby in

8    3/5 cases no or hardly any engraftment was observed at all in the mouse bone marrow

9    compartment. When scaffolds were coated with mouse MSCs instead of human MSCs, a favorable

10    risk sample failed to engraft, and an intermediate risk sample engrafted less efficiently in primary

11    mice, and not at all in secondary mice. During the course of our studies, Reinisch et al also

12    described that ossicles generated by injecting human MSCs with matrigel in xenograft mice could

13    generate a humanized niche in which leukamia patient samples could engraft more efficiently,

14    including favorable risk PML-RARa samples that are notoriously difficult to engraft in normal

15    NSG mice.[31] These data are nicely in line with ours providing independent confirmation of the

16    robustness of these humanized niche xenograft mouse models, but we also provide evidence that

17    stem cell self-renewal is better preserved in a humanized niche as determined by transcriptome

18    studies and serial transplantations.

19    Obviously, heterogeneity exists between leukemia patients, and we find that some patient samples

20    are more dependent on the presence of a human niche than others. As examples, we extensively

21    studied 2 cases: AML #2 which strongly depended on a humanized environment, and AML #1 for

22    which this was much less the case. Consistently, AML #2 could not engraft when i.v.-injected in

23    mice without human scaffolds, the original patient phenotype defined by flow and transcriptome

1 signatures defined by genome-wide transcriptome studies was better maintained in the human

2 scaffolds, self-renewal properties were better preserved in the human scaffolds, and finally the

3 dominant BCR-ABL/inv(16) clone that was present in the original patient sample also grew out in

4 humanized scaffolds while in the mouse bone marrow this clone was absent and instead an minor

5 clone carrying e.g. an IDH1 mutation expanded. Similar observations were published by others[32],

6 showing that upon transplantation of AML samples in NSG or even NSG-SGM3 mice clonal drift

7 can occur, stressing the need for careful genomic analysis of engrafted clones. At the other end of

8 the spectrum, AML #1 could also engraft when injected i.v. into mice without human scaffolds, the

9 original patient phenotype defined by flow and transcriptome signatures was more comparable

10 between human and murine niches, and secondary engraftment could be achieved with muBM-

11 harvested cells as well, albeit with lower frequencies as compared to huBM scaffold-retrieved cells.

12 Overall, our data indicate that the humanized scaffold models will serve as an excellent resource

13 for future studies aimed at exploring novel therapeutic approaches. Experiments were carried out

14 independently in 2 institutes using 2 different mouse strains, NSG and RAG2$^{-/-}$γc$^{-/-}$ mice, showing

15 the robustness of the model. Clinical trials often fail when evaluating drugs that appeared

16 successful in *in vitro* and *in vivo* studies[33,34], and in part this might be related to the models used,

17 whereby a humanized environment was not included. Finally, the current model allows for an

18 efficient evaluation of drug efficacy as well, as already documented for multiple myeloma [18] and

19 MLL-AF9 models[35], indicating that the human leukemia xenograft mouse models that we have

20 established here will serve as an excellent resource for future studies aimed at exploring novel

21 therapeutic approaches.

22

23 **Acknowledgements**

6

**7    Author Contributions**

8    Conceptual design of experiments JJS and RWJG; mouse studies at the UMCG (Groningen, NL)

9    were performed by AA, JJ and JJS; mouse studies at the VU (Amsterdam, NL) were performed by

10    WAN, RdJK, LLA, ACMM, and RWJG; JFvV and ACB analyzed FACS-data; transcriptome

11    studies were performed and analyzed by AZBV and JJS; scaffold material was provided by HY

12    and JDB; AA, BdB, WAN, GJO, EV, ACMM, RWJG and JJS analyzed data; AA, RWJG and JJS

13    wrote the manuscript.

14

15    **Disclosure of Conflicts of Interest:** The authors declare no conflicts of interest.

16

17

# References

Reference List

1. Vargaftig J, Taussig DC, Griessinger E, et al. Frequency of leukemic initiating cells does not depend on the xenotransplantation model used. *Leukemia*. 2011;26(4):858-860.

2. Sanchez PV, Perry RL, Sarry JE, et al. A robust xenotransplantation model for acute myeloid leukemia. *Leukemia*. 2009;23(11):2109-2117.

3. Wunderlich M, Chou FS, Link KA, et al. AML xenograft efficiency is significantly improved in NOD/SCID-IL2RG mice constitutively expressing human SCF, GM-CSF and IL-3. *Leukemia*. 2010;24(10):1785-1788.

4. Barabe F, Kennedy JA, Hope KJ, Dick JE. Modeling the initiation and progression of human acute leukemia in mice. *Science*. 2007;316(5824):600-604.

5. Horton SJ, Jaques J, Woolthuis C, et al. MLL-AF9-mediated immortalization of human hematopoietic cells along different lineages changes during ontogeny. *Leukemia*. 2012;51116-1126.

6. Rizo A, Horton SJ, Olthof S, et al. BMI1 collaborates with BCR-ABL in leukemic transformation of human CD34+ cells. *Blood*. 2010;116(22):4621-4630.

7. Wei J, Wunderlich M, Fox C, et al. Microenvironment determines lineage fate in a human model of MLL-AF9 leukemia. *Cancer Cell*. 2008;13(6):483-495.

8. Townsend EC, Murakami MA, Christodoulou A, et al. The Public Repository of Xenografts Enables Discovery and Randomized Phase II-like Trials in Mice. *Cancer Cell*. 2016;29(4):574-586.

9. Nicolini FE, Cashman JD, Hogge DE, Humphries RK, Eaves CJ. NOD/SCID mice engineered to express human IL-3, GM-CSF and Steel factor constitutively mobilize engrafted human progenitors and compromise human stem cell regeneration. *Leukemia*. 2004;18(2):341-347.

10. Feuring-Buske M, Gerhard B, Cashman J, Humphries RK, Eaves CJ, Hogge DE. Improved engraftment of human acute myeloid leukemia progenitor cells in beta 2-microglobulin-deficient NOD/SCID mice and in NOD/SCID mice transgenic for human growth factors. *Leukemia*. 2003;17(4):760-763.

11. Goyama S, Wunderlich M, Mulloy JC. Xenograft models for normal and malignant stem cells. *Blood*. 2015.

12. Rongvaux A, Willinger T, Martinek J, et al. Development and function of human innate immune cells in a humanized mouse model. *Nat.Biotechnol*. 2014;32(4):364-372.

13. Rongvaux A, Willinger T, Takizawa H, et al. Human thrombopoietin knockin mice efficiently support human hematopoiesis in vivo. *Proc.Natl.Acad.Sci.U.S.A.* 2011;108(6):2378-2383.

14. Strowig T, Rongvaux A, Rathinam C, et al. Transgenic expression of human signal regulatory protein alpha in Rag2-/-gamma(c)-/- mice improves engraftment of human hematopoietic cells in humanized mice. *Proc.Natl.Acad.Sci.U.S.A.* 2011;108(32):13218-13223.

15. Willinger T, Rongvaux A, Takizawa H, et al. Human IL-3/GM-CSF knock-in mice support human alveolar macrophage development and human immune responses in the lung. *Proc.Natl.Acad.Sci.U.S.A.* 2011;108(6):2390-2395.

16. Willinger T, Rongvaux A, Strowig T, Manz MG, Flavell RA. Improving human hemato-lymphoid-system mice by cytokine knock-in gene replacement. *Trends Immunol.* 2011;32(7):321-327.

17. Theocharides AP, Rongvaux A, Fritsch K, Flavell RA, Manz MG. Humanized hemato-lymphoid system mice. *Haematologica*. 2016;101(1):5-19.

18. Groen RW, Noort WA, Raymakers RA, et al. Reconstructing the human hematopoietic niche in immunodeficient mice: opportunities for studying primary multiple myeloma. *Blood*. 2012;120(3):e9-e16.

19. Gutierrez A, Pan L, Groen RW, et al. Phenothiazines induce PP2A-mediated apoptosis in T cell acute lymphoblastic leukemia. *J.Clin.Invest*. 2014;124(2):644-655.

20. Schuringa JJ, Chung KY, Morrone G, Moore MA. Constitutive activation of STAT5A promotes human hematopoietic stem cell self-renewal and erythroid differentiation. *J.Exp.Med.* 2004;200(5):623-635.

21. Schuringa JJ and Schepers H. Ex vivo assays to study self-renewal and long-term expansion of genetically modified primary human acute myeloid leukemia stem cells. *Methods Mol.Biol.* 2009;538287-300.

22. Sontakke P, Carretta M, Capala M, Schepers H, Schuringa JJ. Ex vivo assays to study self-renewal, long-term expansion, and leukemic transformation of genetically modified human hematopoietic and patient-derived leukemic stem cells. *Methods Mol.Biol.* 2014;1185195-210.

23. van Gosliga D, Schepers H, Rizo A, van der Kolk D, Vellenga E, Schuringa JJ. Establishing long-term cultures with self-renewing acute myeloid leukemia stem/progenitor cells. *Exp.Hematol.* 2007;35(10):1538-1549.

24. Calvi LM and Link DC. The hematopoietic stem cell niche in homeostasis and disease. *Blood*. 2015;126(22):2443-2451.

25. Calvi LM, Adams GB, Weibrecht KW, et al. Osteoblastic cells regulate the haematopoietic stem cell niche. *Nature*. 2003;425(6960):841-846.

26. Zhang J, Niu C, Ye L, et al. Identification of the haematopoietic stem cell niche and control of the niche size. *Nature*. 2003;425(6960):836-841.

27. Mendez-Ferrer S, Michurina TV, Ferraro F, et al. Mesenchymal and haematopoietic stem cells form a unique bone marrow niche. *Nature*. 2010;466(7308):829-834.

28. Schepers K, Campbell TB, Passegue E. Normal and leukemic stem cell niches: insights and therapeutic opportunities. *Cell Stem Cell*. 2015;16(3):254-267.

29. Enver T, Pera M, Peterson C, Andrews PW. Stem cell states, fates, and the rules of attraction. *Cell Stem Cell*. 2009;4(5):387-397.

30. Eaves CJ. Hematopoietic stem cells: concepts, definitions, and the new reality. *Blood*. 2015;125(17):2605-2613.

31. Reinisch A, Thomas D, Corces MR, et al. A humanized bone marrow ossicle xenotransplantation model enables improved engraftment of healthy and leukemic human hematopoietic cells. *Nat.Med.* 2016.

32. Klco JM, Spencer DH, Miller CA, et al. Functional heterogeneity of genetically defined subclones in acute myeloid leukemia. *Cancer Cell*. 2014;25(3):379-392.

33. Alizadeh AA, Aranda V, Bardelli A, et al. Toward understanding and exploiting tumor heterogeneity. *Nat.Med.* 2015;21(8):846-853.

34. Gould SE, Junttila MR, de Sauvage FJ. Translational value of mouse models in oncology drug development. *Nat.Med.* 2015;21(5):431-439.

35. Sontakke P, Carretta M, Jaques J, et al. Modeling BCR-ABL and MLL-AF9 leukemia in a human bone marrow-like scaffold based xenograft model. *Leukemia*. 2016;in press.

**Figures Legends**

**Figure 1. Overview of the mouse xenograft leukemia models. A,** Schematic representation of the generation of muBM-iv and huBM-sc models. **B,** Representative HE stain of scaffold sections 6 weeks after implantation; b, bone; s, scaffold; v, blood vessels. **C,** Success rate of leukemia development in muBM-iv and huBM-sc models, expressed as percentage of AML samples from

1   different risk groups, which engrafted or not in the two xenograft models. **D**, Scatter plots showing

2   engraftment of donor human CD45$^+$ cells in different compartments of the mouse at sacrifice

3   (huBM-sc, humanized scaffolds; muBM, murine bone marrow; muSp, murine spleen; muLv,

4   murine liver; muPB, murine peripheral blood). Engraftment values from several mice for each

5   AML sample are expressed as mean±SEM. Route 1: cells were directly injected into the humanized

6   scaffolds, route 2: cells were injected i.v. in mice without humanized scaffolds. **E**, Experiment as in

7   (d), but now cells were injected i.v. in mice carrying humanized scaffolds. **F**, *In vivo* tumor growth

8   rates of the biggest tumor scaffold of each mice. Each colored line represents one mouse from a

9   certain AML sample. Tumor size (cm$^3$) was used as endpoint of the experimental period.

10

11   **Figure 2. Mouse xenograft AML model using sample AML #2. A**, FACS immunophenotype of

12   AML #2 patient-derived MNCs cells. **B,** Representative photograph depicting the "leukemic

13   masses" formed around the extramedullary bones of Sc1 and Sc3 and two scaffolds with no tumor

14   growth (Sc4, not injected control scaffold), at mouse sacrifice. **C**, Representative FACS phenotype

15   from a primary huBM-sc mouse (m23, see Table S1) transplanted with AML #2 cells. Expression

16   of a panel of hematopoietic markers in huCD45$^+$ gated cells isolated from different scaffolds or

17   from the murine BM. **D**, Bar graph summarizing the FACS phenotype of human CD45$^+$ cells from

18   different compartments of all mice injected with #2 AML cells, compared with original patient

19   phenotype. Values are expressed as mean±SEM. **E**, Histologic sections of scaffold tumor from a

20   representative #2 huBM-sc mouse (m24, Sc1) stained with HE, anti-huCD45 or anti-huCD33

21   antibodies. **F**, Representative images (m23) of May Grünwald Giemsa (MGG)-stained

22   cytospins of cells retrieved from Sc1, Sc3 or BM.

23

1 **Figure 3. Assessment of the self-renewal potential of engrafting AML cells by serial**

2 **transplantation of three AML samples. A,** Setup of secondary transplantation experiments.

3 HuCD45$^+$ cells harvested from from a scaffold or from the BM of primary huBM-sc mice were

4 injected in the scaffolds of secondary recipient NSG mice implanted with the humanized niches 6-8

5 weeks before the transplantation of leukemic cells. **B,D,F**, Representative FACS analysis of

6 secondary recipient mice of AML #2, AML #3 and AML #1, respectively. **C,E,G**, *In vivo* tumor

7 growth rates of the biggest tumor scaffold in secondary transplanted mice from AML #2, AML #3

8 and AML #1, respectively . Each colored line represents one mouse and the cell dosage and source

9 (SC=human scaffold or BM=mouse bone marrow) are depicted in the corresponding legend.

10 Tumor size (cm$^3$) was used as endpoint of the experimental period.

11

12 **Figure 4. Assessment of the self-renewal potential of engrafting AML cells by serial**

13 **transplantation of three AML samples. A**, Schematic representation of the generation of mouse

14 models with scaffolds coated with human MSCs (huBM-sc) versus murine MSCs (muBM-sc). **B**,

15 Plots showing % engraftment of donor human CD45$^+$ cells in the scaffolds in huBM-sc versus

16 muBM-sc models, using patient samples with adverse, intermediate and favorable risk.

17 Engraftment values from 8 scaffolds in 2 mice (mouse 1 indicated with red symbols and mouse 2

18 indicated with black symbols) for each AML sample are expressed as mean±SEM. **C**, For

19 secondary transplantations, leukemic cells harvested from the scaffold of a primary huBM-sc or

20 muBM-sc mouse were injected in the scaffolds of secondary recipient huBM-sc or muBM-sc mice.

21 Kaplan Meijer plots are shown. Significant better secondary engraftment for the intermediate risk

22 sample #18 was shown in the huBM-sc model, while significant better engraftment for the

23 favorable risk sample (#33) was already observed in the primary transplantations. **D**, Ceramic

1    scaffold implants coated with murine MSCs generate an ectopic hematopoietic niche.  HE stains of

2    different murine implants, before inocculation with AML. As shown the scaffolds (s) are covered

3    by murine bone (b) with vascularization (v), resulting in the support of the murine hematopoiesis in

4    Rag2-/-γc-/- mice.

5

6    **Figure 5. *In vivo* and *in vitro* maintenance of the genetic heterogeneity of the original AML**

7    **patient samples.** Exome sequencing to determine variant allele frequency in the leukemic

8    populations for 3 representative AML samples: **A**, #2, **B**, #1, **C**, #3. Vertical axis shows the

9    percentage of variant reads per allele, corresponding to different somatic mutations indicated in the

10   legend. On the horizontal axis, several samples from same AML are depicted. All samples were

11   sorted for huCD45 expression before sequencing. VAF around 50% indicated clonal mutations

12   with heterozygous configuration. VAF around 100% would indicate clonal mutations with

13   homozigous configuration, whilst frequencies lower than 50% show the presence of subclonal

14   mutations.

15

16   **Figure 6. Gene expression profiling of patient derived-AML cells and engrafted in the**

17   **humanized or murine hematopoietic niche of huBM-sc mice. A**, Unsupervised hierarchical

18   cluster analysis (Pearson uncentered absolute distance, average linkage)  on gene expression

19   profiles of muBM- or huSC-engrafted huCD45$^+$ cells or patient- derived (MNCs or CD34$^+$)

20   leukemic cells from six different AMLs.  **B**, Supervised cluster with Euclidean distance and ward

21   linkage analyses per AML using genes that were differentially expressed between huBM-sc and

22   muBM-retrieved cells (fold change (FC) ≥ 3). **C**, GO analyses on genes that were differentially

23   expressed between huBM-sc and muBM-retrieved cells (fold change (FC) ≥ 3). **D**, GSEA analyses

1    on genes that were differentially expressed between huBM-sc and muBM-retrieved cells (fold

2    change (FC) ≥ 3). **E**, Expression of individual stem cell-related genes in the diagnostic patient

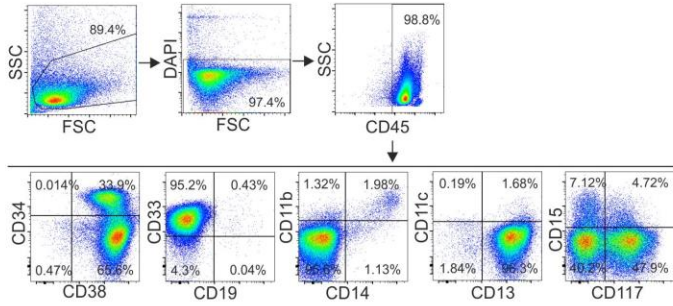3    sample and huBM-sc and muBM-retrieved cells.
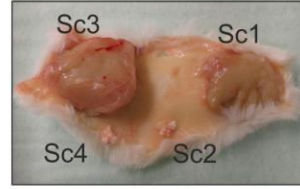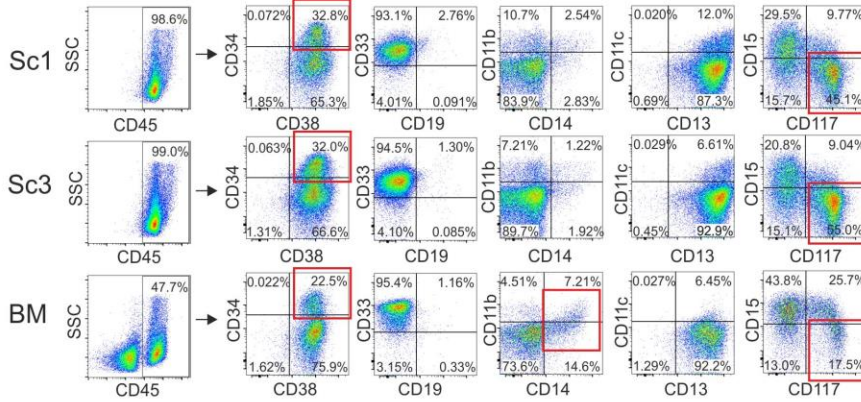
4

# 1 **Figures**

# Fig. 1

**A**



muBM-iv model

huBM-sc model

**B**



**C**



**D**



**E**



**F**
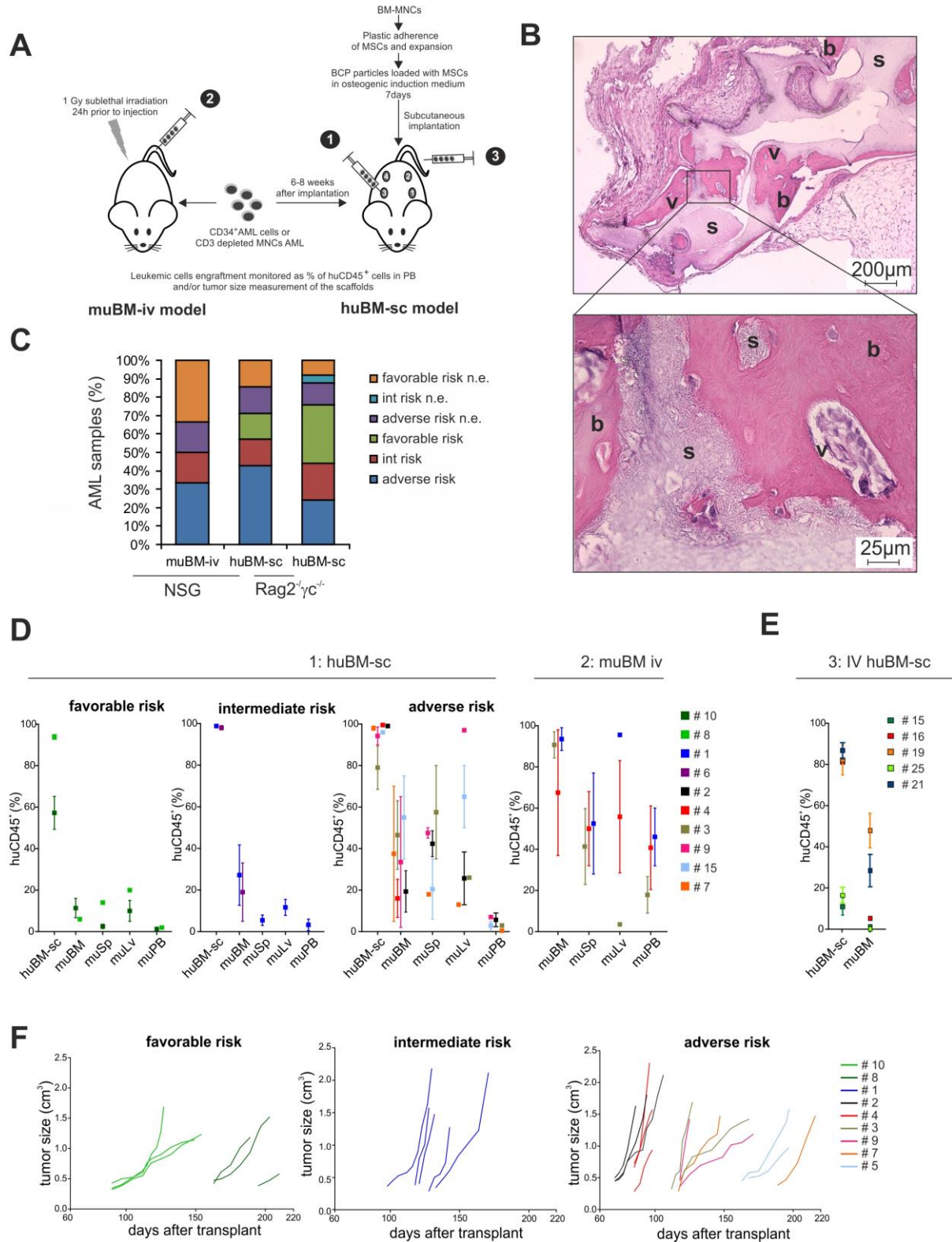


2

# Fig. 2

**A** #2 MNCs



**B** #2 huBM-sc m23



**C** #2 huBM-sc m23



**D**
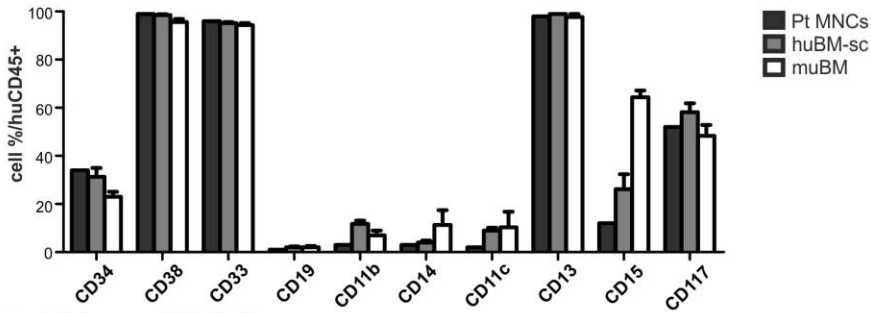


**E** #2 huBM-sc m24 Sc1



**F** #2 huBM-sc m23



1

# Fig. 3

**A** 1st huBM-sc → 2nd huBM-sc          1st muBM → 2nd huBM-sc



**B** #2 huBM-sc
m23.5  week 17          1st huBM-sc → 2nd huBM-sc



1st muBM → 2nd huBM-sc: no engraftment

**C**


23.1 3x10^6 cells SC to SC
23.2 | 10^6 cells SC to SC
23.3 |
23.4 10^5 cells  SC to SC
23.5 4x10^5 cells SC to SC
23.6 10^5 cells  BM to SC
23.7 4x10^5 cells BM to SC

**D** #3 huBM-sc
m26.4  week 31          1st huBM-sc → 2nd huBM-sc



1st muBM → 2nd huBM-sc: no engraftment

**E**


26.1 |
26.2 1.5x10^6 cells SC to SC
26.3 |
26.4 10^5 cells  SC to SC
26.5 3.36x10^5 cells SC to SC
26.6 10^5 cells  BM to SC
26.7 3.36x10^5 cells BM to SC

**F** #1 huBM-sc
m3.8  week 24.5          1st huBM-sc → 2nd huBM-sc



#1 huBM-sc
m3.10  week 35          1st muBM → 2nd huBM-sc



**G**


3.1 | 10^5 cells SC to SC
3.2 |
3.3 3x10^5 cells SC to SC
3.4 | 3x10^5 cells SC to SC
3.5 10^6 cells SC to SC
3.6 |
3.7 4.5x10^5 cells SC to SC
3.8 1.8x10^5 cells SC to SC
3.9 4.5x10^5 cells BM to SC
3.10 1.8x10^5 cells BM to SC

1

29

# Fig. 4

## Fig. 5

# Fig.6